

Synthesis of Arylmethylene-bis(3-hydroxy-5,5-dimethylcyclohex-2-en-1-one) Derivatives and Their Effect on Tyrosinase Activity

Elma Veljović,¹ Hrvoje Rimac,² Mirsada Salihović,^{1,*} Selma Špirtović-Halilović,¹ Amar Osmanović,¹ Nejra Kovač,^{1,3} Elizabeta Kiršek,² Enida Članjak-Kudra,⁴ Dijana Špirtović,⁵ Mirza Bojić²

¹ University of Sarajevo, Faculty of Pharmacy, Zmaja od Bosne 8, 71000 Sarajevo, Bosnia and Herzegovina

² University of Zagreb, Faculty of Pharmacy and Biochemistry, Department of Medicinal Chemistry, Ante Kovačića 1, 10000 Zagreb, Croatia

³ Quality Assurance and Quality Control Department, Bosnalijek d.d., Jukićeva 53, 71000 Sarajevo, Bosnia and Herzegovina

⁴ University of Sarajevo, Veterinary Faculty, Zmaja od Bosne 90, 71000 Sarajevo, Bosnia and Herzegovina

⁵ Clinical Centre of the University of Sarajevo, Department of Clinical Pathology, Cytology and Human Genetics, Bolnička 25, 71000 Sarajevo, Bosnia and Herzegovina

* Corresponding author's e-mail address: mirsada.salihovic@ffsa.unsa.ba

RECEIVED: December 4, 2021 * REVISED: March 3, 2022 * ACCEPTED: March 7, 2022

Abstract: The objective of this study was to test the inhibitory effect of five newly synthesized arylmethylene-bis(3-hydroxy-5,5-dimethylcyclohex-2-en-1-one) derivatives. The structural characterization and stereochemistry of synthesized compounds were deduced from analyses of experimental FT-IR, ¹H, ¹³C NMR spectra and theoretical methodology of DFT study based on the global chemical reactivity indices calculated using the 6-31G** level of theory.

To predict the stability of the newly synthesized compounds, the reactivity descriptors obtained at B3LYP level (E_{gap} , dipole moment, μ , η , ω) were computed. The docking study and the selected quantum chemical descriptors computed for compounds **1–5** exhibit a good agreement. The strongest inhibitors showed 25 to 30 % inhibition of tyrosinase activity. Results were supported by docking studies of the binding of the strongest inhibitors to the enzyme. The results suggest that tetraketones of this type, due to their tyrosinase inhibitory effect, represent potential agents in the treatment of various types of melanomas and skin hyperpigmentation.

Keywords: solubility prediction, NADES, mediterranean herbs, COSMO-RS, choline chloride, eutectic, extraction.

INTRODUCTION

TYROSINASE is an organometallic enzyme involved in the biosynthesis of pigment melanin. Consequently, by increasing or decreasing the level of melanin pigment, tyrosinase is indirectly responsible for a number of clinical disorders.^[1–3] Increased production and accumulation of melanin leads to hyperpigmentation (hypermelanosis), which is associated with many diseases such as melasma, post-inflammatory melanoderma, effelids, lentigines, elderly spots, etc. Epidermal and dermal hyperpigmentation may depend on the increase in the number of melanocytes or the activity of melanogenic enzymes. UV radiation, chronic inflammation, skin rubbing and abnormal release of α -MSH

are the triggers of these disorders. Hyperpigmentation mainly occurs on photoexposed parts (face, hands, upper torso) causing psychosocial and aesthetic problems.^[4–6] Although melanin is primarily responsible for skin color, it also has a protective role against photocarcinogenesis.^[7] Lighter skin contains more pheomelanin and is therefore more susceptible to damage caused by UV radiation. Exposure to UV rays leads to increased production of melanin, but it can also damage melanocytes, which then grow uncontrollably into tumors. Skin cancer is the most common form of cancer with a prevalence of at least 40 %.^[5,8] Currently, there are three main types of skin cancer: squamous cell carcinoma, basal cell carcinoma and melanoma.^[9,10]

Melanoma accounts for less than 2 % of all malignant skin tumors. However, it is the most aggressive form with a death rate of about 75 %.^[11] In order to develop treatment with a cytotoxic response, it is necessary to interfere with the tyrosinase-mediated biosynthetic pathway of the conversion of L-tyrosine to melanin. This may lead to the selective conversion of a tyrosinase-modeling inactive pro-drug modeling tyrosinase into a cytotoxic drug in melanoma cells. This selective strategy in the treatment of malignant melanoma is called melanocyte-directed enzyme prodrug therapy and allows for high drug selectivity in the system.^[12]

As tyrosinase is the most important enzyme in the process of melanogenesis, it has long been a target for the development of melanocytotoxic skin lightening agents.^[13] The immunogenic tyrosinase enzyme has been presented as a sensitive marker of melanoma. Due to the overexpression of melanin mainly restricted in melanocytes during tumorigenesis, tyrosinase is a potential molecular target in melanoma therapy.^[14–17]

Tetraketones (2,2'-arylmethylene-bis(3-hydroxy-5,5-dimethyl-2-cyclohexen-1-one)) represent an important class of compounds that have shown beneficial pharmacological effects *in vitro* (Figure 1). They are widely used as important precursors in the synthesis of various acridindiones as laser dyes and some heterocyclic compounds, xanthendiones and thioxanthenes.^[18,19] Tetraketones exhibit antioxidant, antibacterial and antiviral effects.^[20–22] These compounds are well studied as the inhibitors of the enzyme lipoxygenase.^[23] However, data on studies on their inhibitory effect on tyrosinases are limited.^[18]

Thus, the objective of this study was to assess inhibitory effect of five newly synthesized arylmethylene-bis(3-hydroxy-5,5-dimethyl-2-cyclohexen-1-one) derivatives on the tyrosinase enzyme. Experimental data analyses and theoretical DFT study^[24–27] were used to perform structural characterisation and stereochemistry of the newly synthesized compounds. Theoretical study was performed by using reactivity descriptors and docking study that could help in understanding the chemical behavior of such compounds. In the future, these calculated parameters could be useful in understanding and predicting the behavior of structurally similar compounds of unknown reactivity.

EXPERIMENTAL

Materials and Methods

GENERAL METHOD FOR THE SYNTHESIS OF ARYLMETHYLENE-BIS(3-HYDROXY-5,5-DIMETHYLCYCLOHEX-2-EN-1-ONE) DERIVATIVES (1–5)

A mixture of benzaldehyde (1 mmol), 5,5-dimethylcyclohexane-1,3-dione (2 mmol) and diazobicyclo [2.2.2] octane (DABCO) (0.05 g) in water (20 mL) was refluxed. The flow

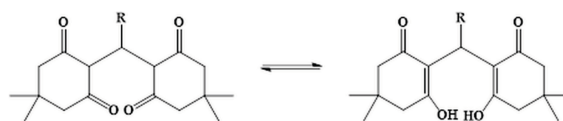


Figure 1. Tetraketones and their keto-enol tautomeric forms.

and completion of the reaction were monitored by thin layer chromatography. After completion of the reaction, the mixture was cooled to room temperature, filtered and washed with water. Recrystallization of the resulting compounds was performed from 95 % ethanol.^[28] All chemicals were obtained from Merck (Germany).

CHARACTERIZATION OF SYNTHETISED PRODUCTS

Elemental Analysis

For the synthesized arylmethylene-bis-(3-hydroxy-5,5-dimethylcyclohex-2-en-1-one) derivatives, elemental analysis was performed with the Vario EL apparatus III C, H, N, S / O Elemental Analyzer, Elementar Analysensysteme GmbH, Hanau-Germany.

IR Spectroscopy

IR spectra of the synthesized compounds were recorded using Shimadzu IR Prestige 21 apparatus in the wavelength range from 4500 to 700 cm^{-1} .

NMR

^1H -NMR and ^{13}C -NMR spectra for the synthesized compounds were recorded with the Bruker AC 250 E apparatus, in deuterated chloroform using TMS (tetramethylsilicon) as a reference standard.

Melting Point

The melting points of the synthesized compounds were determined with the Melting point meter apparatus, manufactured by Kruss optronic, Germany.

DETERMINATION OF TYROSINASE ENZYME ACTIVITY

Five derivatives of arylmethylene-bis(3-hydroxy-5,5-dimethylcyclohex-2-en-1-one) were tested for their ability to inhibit conversion of L-DOPA to dopaquinone and dopachrome by the tyrosinase enzyme. Formation of dopachrome was measured spectrophotometrically at $\lambda = 475 \text{ nm}$. Kojic acid, as a known inhibitor of the tyrosinase enzyme, was used as a positive control. Final concentrations of compounds were as follows: L-DOPA 0.3 mg mL^{-1} , tyrosinase 0.1 mg mL^{-1} , substrates 60 μM . Reactions were conducted at room temperature and dopachrome absorbance was measured every minute for 15 minutes in presence and in absence of inhibitors. All experiments were conducted in triplicate at pH 7.4 and activity of the tyrosinase enzyme without inhibitors was measured daily. Tyrosinase inhibition is defined as the ratio of dopachrome absorbance in presence and in absence of an inhibitor, given as a percentage. All chemicals used in this essay were obtained from Sigma Aldrich (USA).

PHYSICOCHEMICAL PROPERTIES CALCULATIONS

In order to explore the agreement between theoretical and experimental data, quantum chemical calculations were performed with complete geometry optimizations using Spartan 14 software.^[29] Geometry optimization was carried at B3LYP/6-31G** level of theory. The reactivity of compounds **1–5** can be elucidated by computation using global chemical reactivity indices. The chemical reactivity descriptors^[24–27] calculated using DFT were:

- Chemical hardness (η) associated with the stability and reactivity of a chemical system and can be calculated using the following equation:
$$\eta = (\varepsilon_{\text{LUMO}} - \varepsilon_{\text{HOMO}}) / 2;$$
- Electronic chemical potential (μ), defined as the negative of electronegativity of a molecule and can be calculated using equation: $\mu = (\varepsilon_{\text{HOMO}} + \varepsilon_{\text{LUMO}}) / 2;$
- Global electrophilicity index (ω) is calculated using the electronic chemical potential and chemical hardness as shown in equation: $\omega = \mu^2 / 2\eta.$

DOCKING STUDY

Lamarckian Genetic Algorithm of the AutoDock 4.0 program was used to perform the flexible-ligand docking studies.^[30] Receptors' X-ray crystal structures obtained from the Brookhaven protein data bank were applied in docking studies (<http://www.pdb.org/>). Prior to actual docking run, AutoGrid 4.0 was introduced to precalculate grid maps of interaction energies of various atom types. In all dockings, a grid map with $126 \times 126 \times 126$ points, and a grid spacing of 0.6 \AA were used. In an AutoGrid procedure, the protein is embedded in a 3D grid and a probe atom is placed at each grid point. The energy of interaction of this single atom with the protein is assigned to the grid point. AutoDock 4.0 uses these interaction maps to generate ensemble of low energy conformations. It uses a scoring function based on AMBER force field and estimates the free energy of binding of a ligand to its target. For all dockings, 10 independent runs with step sizes of 0.2 \AA for translations and 5 \AA for orientations and torsions, an initial population of random individuals with a population size of 150 individuals, a maximum number of 2500000 energy evaluations and 27000 maximum generations.

Interactions between docked potent agents and related macromolecule were analyzed using AutoDock Tools program (ADT, Version 1.5.4) and PyMol-1.1 software was used for graphical visualization, interactions analysis of ligands and receptors and generating figures.^[31] As the receptor we used tyrosinase from Protein Data Bank (pdb: 1WXC). To gain further insight into binding of best and worst inhibitors to the tyrosinase enzyme, a docking study was performed using AutoDock Vina (The Scripps Research

Institute, La Jolla, CA, USA),^[32] which uses dispersion, hydrogen bonds, and electrostatic and desolvation energy components to determine the conformation of the most probable complex. The three-dimensional coordinates of tyrosinase enzyme molecule, was obtained from RCSB (PDB entry 2Y9W).^[33] Chain A of the crystallographic structure was used due to it being the subunit with the best quality data. The protein molecule was prepared for docking by adding the missing side-chain atoms and hydrogen atoms, all Lys, Arg, His, and Cys sidechains were protonated, all Asp and Glu sidechains were deprotonated, and the amino and carboxy termini were charged. Since there is a presence of a water molecule (HOH 2094) in the vicinity of copper ions, all docking study were performed with both all water molecules removed and all water molecules removed except HOH 2094, as well as with copper ions charged +1 and +2. The three-dimensional forms of the ligands were drawn and their initial geometries were minimized in HyperChem 8.0 (Hypercube, Inc., Gainesville, FL, USA), and their charge was set to represent the most abundant species at pH 7.4, calculated at chemicalize.com and partial charges for ligands were set according to Ionescu et al.^[34] Grid maps of size $22.5 \times 22.5 \times 22.5 \text{ \AA}$ were generated and centered in the tyrosinase active site cavity (4.827, 28.490, 92.879). The receptor molecule was regarded as rigid while all ligand single bonds were allowed to rotate freely during the docking procedure, with exhaustiveness set to 20 and energy range set to 3 kcal mol^{-1} . Since the crystallographic structure of tyrosinase with tropolone molecule is present, docking of tropolone in presence and in absence of HOH 2094 and with copper charge of both +1 and +2 was conducted in order to assess the appropriateness of the system and afterwards docking of L-DOPA, dopaquinone, compound **1**, and kojic acid was conducted using the same conditions.

STATISTICAL ANALYSIS

All incubations were conducted in triplicate. The results are expressed as percentage of enzyme inhibition *i.e.*, percentage of product generated in incubation with the addition of test compound in ratio to the control without the inhibitor. Statistical significance was tested with Student's t-test in the R program (The R Project for Statistical Computing, Vienna, Austria).

RESULTS AND DISCUSSION

Chemistry

New compounds (**1–5**) were synthesized by Knoevenagel condensation of an aromatic aldehyde and Michael addition of 5,5-dimethylcyclohexane-1,3-dione, as shown in Scheme 1.

COMPOUND 1:**2,2'-(4"-TRIFLUOROMETHYLPHENYL)METHYLENE-BIS(3-HYDROXY-5,5-DIMETHYLCYCLOHEX-2-EN-1-ONE**

Yield 74 %; m.p. 186–190 °C; IR(KBr) $\tilde{\nu}_{\max}$ / cm^{-1} : 3000 (Ar-H), 1750 (C=O), 1600(C=C), 1300 (C-O); 1500 (C=O), 1200 (OH), 1100 (C-F); ^1H NMR (CDCl_3) d/ppm : 1.12, 1.24 (ss, 12H, CH-3), 2.23–2.55 (m, 8H, CH-2), 5.54 (s, 1H, CH, C-7), 7.21, 7.54 (dd, 4H, $J = 8.5$ Hz, Ar-H), 11.87 (brs OH disappears with D_2O); ^{13}C NMR (CDCl_3 , d/ppm): 31.41 (C-5 and C-5'), 32.90 (C-7), 46.40 (C-4, C-4'), 47.01 (C-6, C-6'), 115.28 (C-2 and C-2'), 125.70, 125.16, 125.22, 125.27, 127.08 (C-2'', C-3'', C-5'', C-6'', $J_{F,3''} = 3.6\text{Hz}$); 127.31, 127.83, 128.34, 128.86, 142.57 ($J_{F,4''} = 32.4$ Hz), 117.70, 122.02, 126.35, 130.66 (CF_3 , $J_{F,C} = 271.9$ Hz), 189.43, 190.73 (C-3, C-3'). Anal. Calcd. mass fractions of elements, w / %, for $\text{C}_{24}\text{H}_{27}\text{F}_3\text{O}_4$ ($M_r = 439.19$) are: C = 66.04, H = 6.24; found: C = 66.41, H = 6.38.

COMPOUND 2: 2,2'-(4"-ACETAMIDOPHENYL)METHYLENE-BIS(3-HYDROXY-5,5-DIMETHYLCYCLOHEX-2-EN-1-ONE

Yield 68 %; m.p. 171–173 °C; IR(KBr) $\tilde{\nu}_{\max}$ / cm^{-1} : 3050 (Ar-H), 1700 (C=O), 1600(C=C), 1300 (C-O), 1500 (C=O), 1200 (OH), 1620 (amide); ^1H NMR (CDCl_3) d/ppm : 1.09, 1.21 (2 x s, 12H, 4xCH₃), 2.12 (s, NHCOCH₃), 2.20–2.52 (m, 8H, 4CH₂), 5.48 (s 1H, CH), 7.01 (d, 2H, $J_{2,3'} = 9.2$ Hz, H-2', H-6'), 7.40 (d, 2H, $J_{2,3'} = 9.2$ Hz, H-3', H-5'), 7.56 (s, 1H, NHCOCH₃), 11.87 (brs OH disappears with D_2O); ^{13}C NMR (CDCl_3 , d/ppm): 24.45 (NHCOCH₃), 27.31, 29.55 (CH₃ from C(CH₃)₂), 31.34 (C(CH₃)₂), 32.30 (CH), 46.37, 47.00 (CH₂), 115.50 (C-1), 119.56, 127.27 (CH), 133.77, 135.79; 168.29 (NHCOCH₃), 189.35, 190.48 (C-2, C=O). Anal. Calcd. mass fractions of

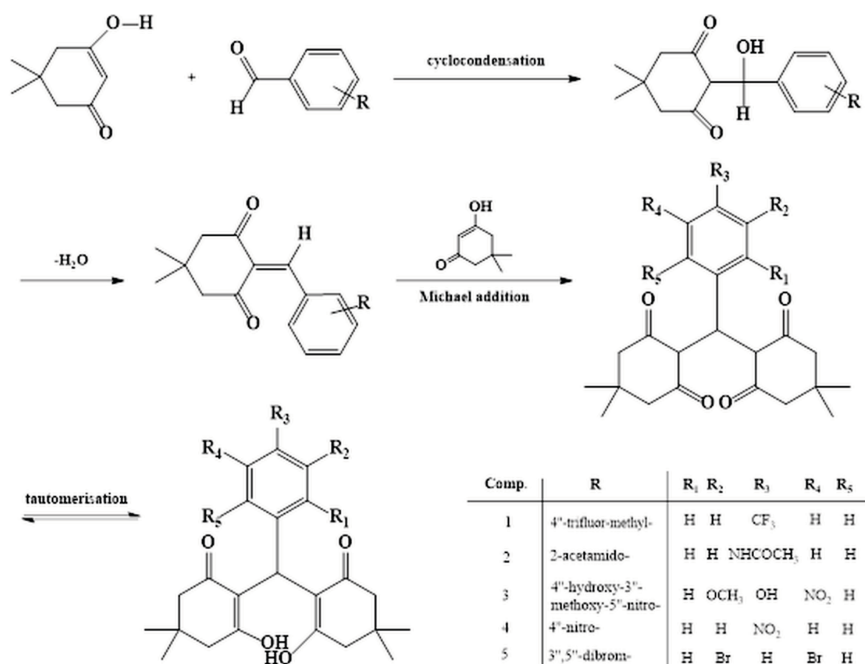
elements, w / %, for $\text{C}_{25}\text{H}_{31}\text{N}_1\text{O}_5$ ($M_r = 425.22$) are: C = 70.57, H = 7.34; found: C = 70.2, H = 7.12.

COMPOUND 3: 2,2'-(4"-HYDROXY-3"-METHOXY-5"-NITROPHENYL)METHYLENE-BIS(3-HYDROXY-5,5-DIMETHYLCYCLOHEX-2-EN-1-ONE

Yield 71 %; m.p. 230–232 °C; IR(KBr) $\tilde{\nu}_{\max}$ / cm^{-1} : 2500–3300 (Ar-OH), 3042 (Ar-H), 1730 (C=O), 1607, 1588 (C=C), 1448 (O-CH₃), 1320 (C-O), 1200 (Ar-OH), 1595 (NO₂); ^1H NMR (CDCl_3) d/ppm : 1.12 (6H, s, H-14, H-16), 1.25 (6H, s, H-15, H-17), 2.22–2.54 (8H, m, H-3, H-11, H-5, H-9), 3.83 (3H, s, OCH₃), 5.43 (1H, s, H-13), 6.90 (1H, s, H-2'), 7.44 (1H, s, H-6'), 10.60 (1H, brs, Ar-OH disappears with D_2O); ^{13}C NMR (CDCl_3 , d/ppm): 26.87 (C-14, C-16), 29.82 (C-15, C-17), 31.39 (C-4, C-10), 33.18 (C-13), 114.01 (C-6'), 117.04 (C-2'), 114.71 (C-1, C-7), 133.60 (C-4'), 144.41 (C-5'), 149.59 (C-3'), 189.45 (C-2, C-12), 190.94 (C-6, C-8). Anal. Calcd. mass fractions of elements, w / %, for $\text{C}_{24}\text{H}_{27}\text{N}_1\text{O}_8$ ($M_r = 457.17$) are: C = 62.73, H = 6.36; found: C = 63.10, H = 6.08.

COMPOUND 4: 2,2'-(4"-NITROPHENYL)METHYLENE-BIS(3-HYDROXY-5,5-DIMETHYLCYCLOHEX-2-EN-1-ONE

Yield 77 %; m.p. 189–203 °C; IR(KBr) $\tilde{\nu}_{\max}/\text{cm}^{-1}$: 3000 (Ar-H), 1670 (C=O), 1480(C=C), 1300 (C-O), 1500 (C=O), 1250 (NO₂); ^1H NMR (CDCl_3) d/ppm : 1.11, 1.23 (2xs, 12H, 4xCH₃), 2.21–2.57 (m, 8H, 4xCH₂), 5.53 (s 1H, CH), 7.24 (d, 2H, $J_{2,3'} = 8.9$ Hz, H-2', H-6') 8.13 (d, 2H, $J_{2,3'} = 8.9$ Hz H-3', H-5'), 11.8 (brs, - OH disappears with D_2O); ^{13}C NMR (CDCl_3 , d/ppm): 27.38, 29.38 (CH₃ from C(CH₃)₂), 31.39 (C(CH₃)₂), 33.18 (CH), 46.32, 46.91 (CH₂), 114.81 (C-1), 123.40, 127.56 (Ar-CH), 146.03, 146.49 (Ar-Cq), 189.46, 190.82 (C-2 and C=O). Anal.



Scheme 1. Synthesis of novel arylmethylene-bis(3-hydroxy-5,5-dimethylcyclohex-2-en-1-one) derivatives.

Calcd. mass fractions of elements, $w / \%$, for $C_{23}H_{27}N_1O_6$ ($M_r = 413.18$) are: C = 66.81, H = 6.58; found: C = 66.74, H = 6.62.

COMPOUND 5: 2,2'-(3'',5''-DIBROMOPHENYL)METHYLENE-BIS(3-HYDROXY-5,5-DIMETHYLCYCLOHEX-2-EN-1-ONE

Yield 69 %; m.p. 248–252 °C; IR(KBr) $\tilde{\nu}_{max} / cm^{-1}$: 3000 (Ar-H), 1750 (C=O), 1600 (C=C), 1300 (C-O), 1400 (C=O), 1220 (OH), 750 (C-Br); 1H NMR ($CDCl_3$) d/ppm : 1.11, 1.23 (ss, 12H, CH_3), 2.10–2.54 (m, 8H, CH_2), 5.44 (s, 1H, CH, C-7), 7.14 (s, 2H, H-2'', H-6''), 7.47 (s, 1H, H-4''), 11.90 (brs OH disappears with D_2O); ^{13}C NMR ($CDCl_3$, d / ppm): 27.25, 29.47 (CH_3 from $C(CH_3)_2$ at C-5 and C-5'), 31.44 (C-5 and C-5'), 32.51 (C-7), 46.34 (C-4, C-4'), 46.95 (C-6, C-6'), 114.54 (C-2 i C-2'), 128.90 (C-4''), 131.47 (C-2'', C-6''), 122.73 (C-3'', C-5''), 142.59 (C-1''), 189.42 (C-3, C-3'), 190.75 (C-1, C-1'). Anal. Calcd. mass fractions of elements, $w / \%$, for $C_{23}H_{26}Br_2O_4$ ($M_r = 524.02$) are: C = 52.49, H = 4.98; found: C = 52.75, H = 5.02.

Influence of Tetraketones on the Tyrosinase Enzyme Activity

Results of the tyrosinase inhibition assay are listed in Table 1. Kojic acid, which was used as a positive control, showed a very high enzyme inhibition of $72 \pm 4 \%$. On the other hand, tested tetraketones showed a much lower tyrosinase inhibitory activity, with compounds **3** ($14 \pm 2 \%$) and **2** ($13 \pm 2 \%$) being the strongest tyrosinase inhibitors. However, this difference in activity is not necessarily a problem, as the use of kojic acid in cosmetics is controversial due to its toxicity and mutagenicity.^[35,36] Similar concerns are raised for another strong and widely used tyrosinase inhibitor, hydroquinone.^[37] It seems that high tyrosinase inhibitory activity is often correlated with higher toxicity, therefore there is still much room left to find tyrosinase inhibitors with good physico-chemical properties, with the tyrosinase inhibitory itself not being the most important parameter. In this regard, the most potent compounds in this research, namely compounds **2** and **3**, can serve as lead compounds for further optimization of the structure, both in the sense of increased tyrosinase inhibitory activity, as well as in the sense of lower toxicity.

Table 1. Tyrosinase activity inhibition in the presence of tetraketones.

Compound	Enzyme inhibition (\pm std. er. in %)
1	2 ± 1
2	13 ± 2
3	14 ± 2
4	3 ± 1
5	10 ± 1
Control: kojic acid	72 ± 4

Theoretical Calculations

PHYSICO-CHEMICAL PROPERTIES CALCULATIONS

Calculated global physicochemical properties are presented in Table 2. The results indicate that the trend in the chemical hardness (η) for the compounds is **1** > **5** > **4** > **2** > **3**. - generally, higher the chemical hardness, the more stable or less reactive the compound is. Therefore, compound **1** is the hardest and least reactive, and compounds **2** and **3** are least hard and most reactive.

The electronic chemical potential (μ), defined as the negative of electronegativity of a molecule, is described as the escaping tendency of electrons from an equilibrium system.^[27] The trend in the electronic chemical potential for the compounds is **2** > **5** > **1** > **3** > **4**. The higher the electronic chemical potential, the less stable or more reactive is the molecule. Therefore, compound **2** is the most reactive, and compound **4** is the least reactive of these compounds.

Electrophilicity (ω) measures the propensity or capacity of a species to accept electrons.^[27] The values ω for compounds **1–5** are presented in Table 2. Among these compounds, compound **2** is the strongest nucleophile because it has the lowest value. Compound **4** is the strongest electrophile because it has the highest value.

Compound **1** has the highest HOMO–LUMO energy gap, which indicates that it is the most stable or the least reactive, compared to compounds **5**, **4**, **2**, and **3**, as shown in Table 2.

Table 2. Global chemical reactivity indices of compounds **1–5** at B3LYP/6-31G** level.

	1	2	3	4	5
E_{HOMO} / eV	-6.67	-5.75	-6.26	-6.78	-6.45
E_{LUMO} / eV	-1.30	-1.12	-2.58	-2.12	-1.41
Dipole moment / Debye	4.55	6.08	3.15	8.31	5.63
Energy gap / eV	5.37	4.63	3.68	4.66	5.01
μ / eV	-3.99	-3.44	-4.42	-4.45	-3.94
η / eV	2.68	2.32	1.84	2.34	2.50
ω / eV	2.97	2.55	5.31	7.37	3.10

Table 3. The correlation factors of compared stretching frequencies and chemical shifts for compounds **1–5**.

Comp.	R^2 for Assignment B3LYP/631G**	R^2 for 1H -NMR B3LYP/631G**	R^2 for ^{13}C -NMR B3LYP/631G**
1	0.9977	0.9892	0.9928
2	0.9985	0.9839	0.9791
3	0.9985	0.9988	0.9788
4	0.9981	0.9649	0.9946
5	1.0000	0.9861	0.9931

The electric dipole moment is a product of the positive charge and the distance between the charges. The magnitude of the dipole moment of the molecule is also provided in the Table 2. The trend in the dipole moment for the compounds is $4 > 2 > 5 > 1 > 3$. A large dipole moment indicates a large separation of charge. Electrical dipole moment in chemistry is suitable for describing many intermolecular interactions because the most interesting ones are usually dipole ones.

Comparison of the experimentally and theoretically obtained stretching frequencies in the IR spectra can be utilized to eliminate the uncertainties in the fundamental assignments of the spectra. The correlation factors of the linear regression used to compare the experimentally measured and theoretically computed IR spectra for compounds 1–5 are presented in Table 3. The calculated and experimentally obtained stretching frequencies values show good correspondence.

Chemical shifts for ^1H - and ^{13}C -NMR calculated using the B3LYP level with the 6-31G* and 631G** basis sets can be utilized to eliminate uncertainties in the fundamental assignments of the spectra. The correlation factors of the linear regression used to compare the experimentally measured and theoretically computed NMR shifts for compounds 1–5 are presented in Table 3. The calculated and experimental chemical shift values given in Table 3 show good correspondence with the DFT study.

DOCKING STUDY

Since all docking results were virtually identical with both presence and absence of HOH 2094 and with Cu charges of +1 and +2, only docking results in absence of all water molecules and charges of both Cu ions of +2 will be shown. The comparison of docked tropolone with the crystallographic structure of tropolone bound to tyrosinase showed high similarity, even though their orientations differ (Figure 2), which is understandable, given the size of the ligand.

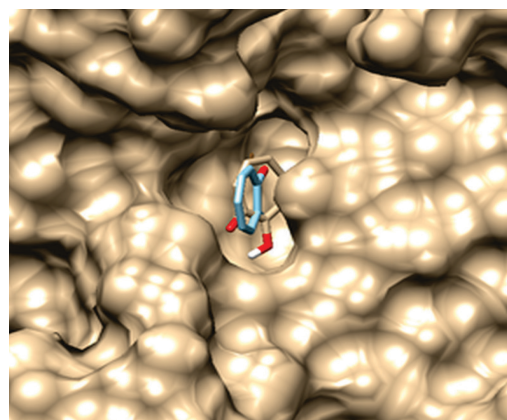


Figure 2. Overlay of the crystallographic structure of tropolone (blue) with docked tropolone (brown) at the cavity of the tyrosinase active site.

Docking of L-DOPA and dopaquinone revealed some interesting characteristics of the area near the binding site. Figure 3a shows the two best (lowest energy) poses of L-DOPA with predicted binding energies of -5.5 and -5.4 kcal mol $^{-1}$, respectively. Figure 3b shows the two best docked poses of dopaquinone, with predicted binding energies of -5.6 and -5.5 kcal mol $^{-1}$. Even though docking programs are known not to be able to accurately predict binding energies,^[4] their relative binding energies can still be compared, especially for different poses of the same molecule. It can be observed that the most favorable L-DOPA binding location is in the active site, with catechol group oriented towards the two Cu $^{2+}$ ions.^[38] As for the dopaquinone molecule, the location with the most favorable binding interactions appears to be outside of the binding pocket, which suggests that the dopaquinone molecule leaves the active site before being further metabolized to dopachrome (Figure 3).

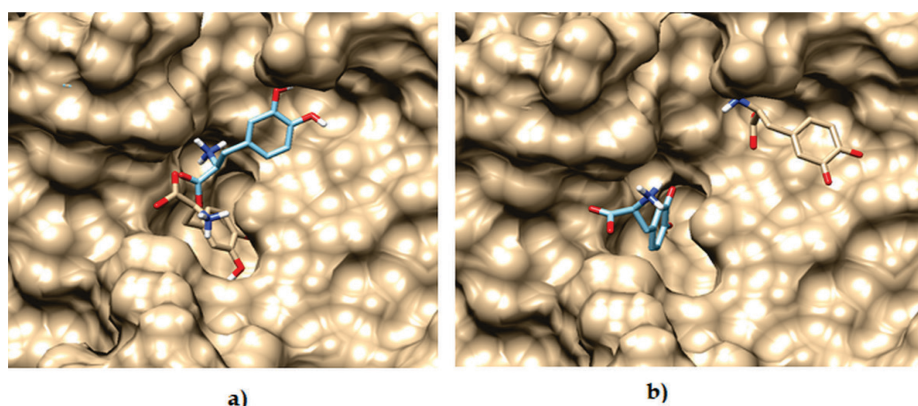


Figure 3. a) Best (brown) and second best (blue) binding poses of L-DOPA to tyrosinase enzyme; b) Best (brown) and second best (blue) binding poses of dopaquinone to tyrosinase enzyme.

The binding site of compound **1** is located at the entrance of tyrosinase, however, it does not protrude into it. Even though the predicted binding energy of the compound **1** ($-6.3 \text{ kcal mol}^{-1}$) is low, its weaker inhibition of the tyrosinase enzyme can be explained by the aforementioned unsatisfactory prediction of binding energies by docking programs, or by its possible short residence time, which allows L-DOPA to be metabolized even in the presence of the inhibitor.^[39,40] Another evidence for inaccurate prediction of binding energies comes from the fact that the binding energy of kojic acid, which should also bind inside the active pocket has predicted energy of $-5.3 \text{ kcal mol}^{-1}$, higher than compound **1** while from the experimental data it can be observed that kojic acid is the most potent inhibitor by a large margin.

Another interesting observation is that the second-best binding poses of the tested inhibitors (compound **1** and kojic acid) are located beside the active pocket (Figure 4 and 5), with similar binding energies as the best poses (-6.3 , and $-5.2 \text{ kcal mol}^{-1}$, respectively), which can serve as a clue for designing even stronger inhibitors, which bind both in the active site and extend into this region and interacting with

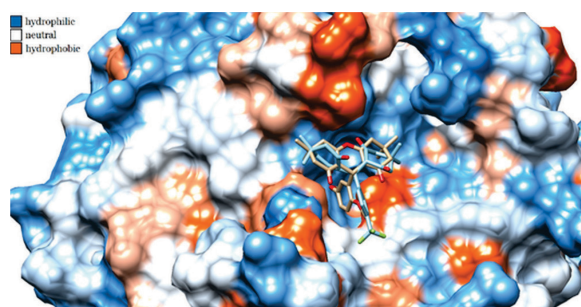


Figure 4. Binding positions of compound **1** (blue) to tyrosinase enzyme. Hydrophilic amino acids are depicted in blue, neutral in white and hydrophobic in red.

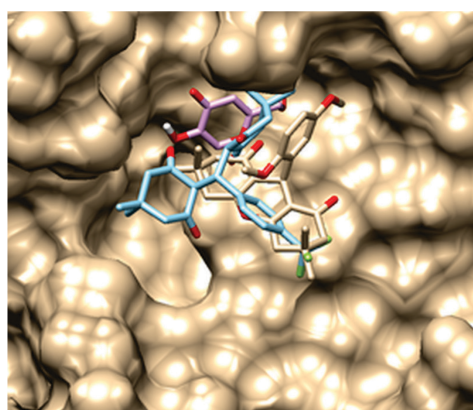


Figure 5. Secondary binding poses of compound **1** (blue), and kojic acid (purple) in the vicinity of the active site.

Table 4. Docking study parameters of synthesized tetraketones.

Comp.	Binding Energy / kcal mol^{-1}	Inhibitory constant / mM	No. of H-bonds	Amino acid
1	-6.48	17.65	1	Val34
2	-7.70	2.28	1	Arg30
3	-6.57	15.24	2	Arg114
4	-7.16	5.63	3	Glu43, Arg85
5	-6.93	8.35	1	Arg228

hydrophilic amino acids in this region, such as Tyr65, Asn81, Cys83, Thr84, His85, His244, Glu322, and Thr324.

For the selected tetraketones, binding energies, inhibitory constants and binding sites of tyrosinase (pdb: 1WXC) were determined and are shown in Table 4. Compound **2** with the acetamido group at *para* position of the phenyl ring in docking studies showed lowest binding energy value ($-7.7 \text{ kcal mol}^{-1}$), as well as the lowest value of the inhibitory constant (2.28 mM). Based on these results, it can be concluded that it has the strongest inhibitory effect on the enzyme tyrosinase, as confirmed by *in vitro* studies (Table 1) where its inhibitory activity of 13 % was second best. Compound **2** forms one hydrogen bond with the tyrosinase enzyme *via* Arg 30. Also, compound **1**, which has a trifluoromethyl group in the *para* position of the phenyl ring, has the highest binding energy ($-6.48 \text{ kcal mol}^{-1}$), as well as the highest inhibitory constant value (17.65 mM), meaning it is the weakest tyrosinase inhibitor. Again, the results of the *in vitro* assays showed good correlation with these results because compound **1** inhibition percentage was only 2 % (Table 1).

CONCLUSION

This study tested a series of newly synthesized arylmethylene-bis(3-hydroxy-5,5-dimethylcyclohex-2-en-1-one) derivatives as tyrosinase inhibitors.

The optimized geometry, IR vibration frequencies, ^1H and ^{13}C NMR chemical shifts, HOMO-LUMO energies, and global indices for the chemical reactivity of the compounds **1–5** were obtained at the B3LYP/6-31G** level of theory using the Spartan 14 program. The theoretical results for ^1H and ^{13}C NMR and FT-IR spectroscopy were reported and compared with experimental data. It was found that the obtained theoretical results for all analyzed compounds were compatible with the experimental data. This theoretical and experimental evidence supports the proposed structures for compounds **1–5**.

The HOMO-LUMO energy gap was highest for compound **1** and lowest for compound **3**. According to calculated results of the electronic chemical potential (μ),

compound **2** (with the acetamido group at *para* position of the phenyl ring) was the least stable (or the most reactive) which is in good accordance with experimental data of *in vitro* tyrosinase inhibition, as well as with results of docking study where compound **2** showed the lowest binding energy and the lowest value of the inhibitory constant.

In conclusion, tetraketones can be regarded as good lead compounds as inhibitors of tyrosinase. Observed experimental data is supported by computational and docking studies. Design of stronger inhibitors should be directed to tetraketones that can bind both in the active site and extend into the region of hydrophilic amino acids.

REFERENCES

- [1] J. Geng, S. Yu, X. Wan, X. Wang, P. Shen, P. Zhou, X. D. Chen, *J. Biochem. Biophys. Methods*. **2008**. *70*, 1151–1155.
<https://doi.org/10.1016/j.jprot.2007.12.013>
- [2] R. J. Obaid, E. U. Mughal, N. Naeem, A. Sadiq, R. I. Alsantali, R. S. Jassas, Z. Moussa, S. A. Ahmed, *RSC Adv*. **2021**. *11*, 22159–22198.
<https://doi.org/10.1039/d1ra03196a>
- [3] S. Yu, M. He, Y. Zhai, Z. Xie, S. Xu, S. Yu, H. Xiao, Y. Song, *Food & Funct.* **2021**. *12*, 2569–2579.
<https://doi.org/10.1039/d0fo03264f>
- [4] W. H. Kang, K. H. Yoon, E.-S. Lee, J. Kim, K. B. Lee, H. Yim, S. Sohn, S. Im, *Br. J. Dermatol.* **2002**. *146*, 228–237.
<https://doi.org/10.1046/j.0007-0963.2001.04556.x>
- [5] A. Prohic, *Dermatovenerology*. 1st ed.; School of Medicine University of Sarajevo: Sarajevo. Bosnia and Herzegovina. **2012**.
- [6] H. Moreiras, M. C. Seabra, D. C. Barral, *Int. J. Mol. Sci.* **2021**. *22*, 4466.
<https://doi.org/10.3390/ijms22094466>
- [7] B. Bellei, A. Pitisci, E. Izzo, M. Picardo, *PLoS ONE* **2012**. *7*, e33021.
<https://doi.org/10.1371/journal.pone.0033021>
- [8] F. P. Noonan, M. R. Zaidi, A. Wolnicka-Glubisz, M. R. Anver, J. Bahn, A. Wielgus, J. Cadet, T. Douki, S. Mouret, M. A. Tucker, A. Popratiloff, G. Merlino, E. C. De Fabo, *Nat. Commun.* **2012**. *3*, 884–894.
<https://doi.org/10.1038/ncomms1893>
- [9] Y. Sang, Y. Deng, *Derm. Ther.* **2019**. *32*, e12964.
<https://doi.org/10.1111/dth.12964>
- [10] D. I. Khodzhaeva, *J of Innovations in Soc. Sci.* **2021**. *1*, 101–104.
<http://sciencebox.uz/index.php/jis/article/view/80>
- [11] M. Rastrelli, S. Tropea, C. R. Rossi, M. Alaibac, *In Vivo*, **2014**. *28*, 1005–1011.
<https://iv.iarjournals.org/content/invivo/28/6/1005.full.pdf>
- [12] M. Rooseboom, J. N. M. Commandeur, N. P. E. Vermeulen, *Pharmacol. Rev.* **2004**. *56*, 53–102.
<https://doi.org/10.1124/pr.56.1.3>
- [13] J. G. Monzon, J. Dancey, *Onco. Targets Ther.* **2012**. *5*, 31–46.
<https://doi.org/10.2147/ott.s21259>
- [14] J. L. Boyle, H. M. Haupt, J. B. Stern, H. A. B. Multhaupt, *Arch. Pathol. Lab. Med.* **2002**. *126*, 816–822.
<https://doi.org/10.5858/2002-126-0816-teimmd>
- [15] A. M. Jordan, T. H. Khan, H. Malkin, H. M. I. Osborn, *Bioorg. Med. Chem.* **2002**. *10*, 2625–2633.
[https://doi.org/10.1016/s0968-0896\(02\)00097-4](https://doi.org/10.1016/s0968-0896(02)00097-4)
- [16] A. J. Vargas, S. Sittadjody, T. Thangasamy, E. E. Mendoza, K. H., *Integr. Cancer Ther.* **2011**. *10*, 328–340.
<https://doi.org/10.1177/1534735410391661>
- [17] S. Jawaid, T. H. Khan, H. M. I. Osborn, N. A. O. Williams, *Anticancer Agents Med. Chem.* **2009**. *9*, 717–727.
<https://doi.org/10.2174/187152009789056886>
- [18] K. M. Khan, G. M. Maharvi, M. T. H. Khan, A. Jabbar Shaikh, S. Perveen, S. Begum, M. I. Choudhary, *Bioorg Med Chem.* **2006**. *14*, 344–351.
<https://doi.org/10.1016/j.bmc.2005.08.029>
- [19] R. Shashi, N. S. Begum, A. K. Panday, *Mol. Cryst. Liq. Cryst.* **2021**. *709*, 81–97.
<https://doi.org/10.1080/15421406.2020.1829308>
- [20] G. M. Maharvi, S. Ali, N. Riaz, N. Afza, A. Malik, M. Ashraf, L. Iqbal, M. Lateef, *J. Enzyme Inhib. Med. Chem.* **2008**. *23*, 62–69.
<https://doi.org/10.1080/14756360701408754>
- [21] A. Fraihat, L. Alatrash, R. Abbasi, B. Abu-Irmaileh, S. Hamed, M. Mohammad, E. Abu-Rish, Y. Bustanji, *Trop. J. Pharm. Res.* *17*, 1081.
<https://doi.org/10.4314/tjpr.v17i6.15>
- [22] L. S. Fernandes, M. L. da Silva, R. S. Dias, M. S. da S. Lucindo, Í. E. P. da Silva, C. C. Silva, R. R. Teixeira, S. O. de Paula, *Viruses*. **2021**. *13*, 2123.
<https://doi.org/10.3390/v13112123>
- [23] S. Ali, G. M. Maharvi, N. Riaz, N. Afza, A. Malik, A. U. Rehman, M. Lateef, L. Iqbal, *West Indian Med. J.* **2009**. *58*, 92–98.
https://www.mona.uwi.edu/fms/wimj/system/files/article_pdfs/ali.pdf
- [24] R. G. Pearson, *Weinheim: Wiley-VCH.* **1997**. *10*.
<http://dx.doi.org/10.1002/3527606173>
- [25] R. G. Parr, R. G. Pearson, *J. Am. Chem. Soc.* **1983**. *105*, 7512–7516.
<https://doi.org/10.1021/ja00364a005>
- [26] A. D. Becke, *J. Chem. Phys.* **1992**. *96*, 2155–2160.
<https://doi.org/10.1063/1.462066>
- [27] C. Lee, W. Yang, R. G. Parr, *Phys. Rev. B.* **1988**. *2013*, 785.
<https://doi.org/10.1103/PhysRevB.37.785>

- [28] P. Paliwal, S. R. Jetti, A. Bhatewara, T. Kadre, S. Jain, *ISRN Org. Chem.* **2013**, 2013, 1–6. <https://doi.org/10.1155/2013/526173>
- [29] Y. Shao, L. F. Molnar, Y. Jung, J. Kussmann, C. Ochsenfeld, S. T. Brown, A. T. Gilbert, L. V. Slipchenko, S. V. Levchenko, D. P. O’Neill, R. A. DiStasio Jr. *Phys. Chem. Chem. Phys.* **2006**, 8, 3172–3191.
- [30] G. M. Morris, R. Huey, W. Lindstrom, M. F. Sanner, R. K. Belew, D. S. Goodsell, A. J. Olson, *J. Comput. Chem.* **2009**, 30, 2785–2791. <https://doi.org/10.1002/jcc.21256>
- [31] M. A. Lill, M. L. Danielson, *J. Comput. Aid. Mol. Des.* **2011**, 25, 13–19. <https://doi.org/10.1007/s10822-010-9395-8>
- [32] O. Trott, A. J. Olson, *J. Comput. Chem.* **2009**, NA-NA. <https://doi.org/10.1002/jcc.21334>
- [33] W. T. Ismaya, H. J. Rozeboom, A. Weijn, J. J. Mes, F. Fusetti, H. J. Wichers, B. W. Dijkstra, *Biochem.* **2011**, 50, 5477–5486. <https://doi.org/10.1021/bi200395t>
- [34] C.-M. Ionescu, D. Sehnal, F. L. Falginella, P. Pant, L. Pravda, T. Bouchal, R. Svobodová Vařeková, S. Geidl, J. Koča, *J. Cheminform.* **2015**, 7, 1–13. <https://doi.org/10.1186/s13321-015-0099-x>
- [35] C. I. Wei, T. S. Huang, S. Y. Fernando, K. T. Chung, *Toxicol. Lett.* **1991**, 59, 213–220. [https://doi.org/10.1016/0378-4274\(91\)90074-G](https://doi.org/10.1016/0378-4274(91)90074-G)
- [36] C. L. Burnett, W. F. Bergfeld, D. V. Belsito, R. A. Hill, C. D. Klaassen, C. D., Liebler, J. G. Marks, R. C. Shank, T. J. Slaga, P. W. Snyder, F. A. Andersen, *Int. J. Toxicol.* **2010**, 29, 244S–273S. <https://doi.org/10.1177/1091581810385956>
- [37] J. J. Nordlund, P. E. Grimes, J. P. Ortonne, *J. Eur. Acad. Dermatol. Venereol.* **2006**, 20, 781–787. <https://doi.org/10.1111/j.1468-3083.2006.01670.x>
- [38] N. Makino, P. McMahill, H. S. Mason, T. H. Moss, *J. Biol. Chem.* **1974**, 249, 6062–6066. [https://doi.org/10.1016/s0021-9258\(19\)42219-9](https://doi.org/10.1016/s0021-9258(19)42219-9)
- [39] P. J. Tummino and R. A. Copeland, *Biochem.* **2008**, 47, 5481–5492. <https://doi.org/10.1021/bi8002023>
- [40] H. Lu, P. J. Tonge, *Curr. Opin. Chem. Biol.* **2010**, 14, 467–474. <https://doi.org/10.1016/j.cbpa.2010.06.176>